minerals

MDPI

Article

Research on the Rapid Strengthening Mechanism of Microwave Field-Controlled Gypsum-Cemented Analog Materials

Senlin Nan [1,2], Wentao Li [1,2], Weiming Guan [1,2,*], Huabin Liu [1,2], Hongchao Zhao [1,2], Yingyuan Wen [1,2] and Junhui Yao [1,2]

[1] College of Geology and Mines Engineering, Xinjiang University, Urumqi 830047, China; nansenlin@stu.xju.edu.cn (S.N.); lwt@stu.xju.edu.cn (W.L.); lhb@stu.xju.edu.cn (H.L.); zhaohongchao@xju.edu.cn (H.Z.); wyyxju@xju.edu.cn (Y.W.); rockman@xju.edu.cn (J.Y.)

[2] Autonomous Region Experimental Teaching Demonstration Center for Geology and Mining Engineering, Xinjiang University, Urumqi 830047, China

* Correspondence: gwmxju@xju.edu.cn; Tel.: +86-1399-919-0583

Abstract: Various geotechnical experiments have used gypsum-cemented analog geotechnical materials. However, this material needs a long curing time, and the target strength is not easy to control. Therefore, this research adopted microwave heating as the curing method for this kind of material. Objectively, the authors investigated the variations in the material strength versus heating power and heating time. On this basis, we clarified the influence mechanism of microwaves on the strength of analog materials by analyzing material temperature, moisture content, and microstructure, which eventually led to an experimental control method for rapid strengthening of microwave field-controlled gypsum-cemented analog materials. Consequently, we drew the following conclusions. The stable strength of the material under high-power microwave curing was much lower than that under natural curing, while the material strength under low-power microwave curing was the closest to the material under natural curing.

Keywords: microwave; gypsum cementation; analog materials; hardening rate; analog physical simulation experiment

Citation: Nan, S.; Li, W.; Guan, W.; Liu, H.; Zhao, H.; Wen, Y.; Yao, J. Research on the Rapid Strengthening Mechanism of Microwave Field-Controlled Gypsum-Cemented Analog Materials. *Minerals* **2021**, *11*, 1348. https://doi.org/10.3390/min11121348

Academic Editor: Carlito Tabelin

Received: 5 November 2021
Accepted: 26 November 2021
Published: 30 November 2021

1. Introduction

China has a huge amount of coal mining, which often causes adverse effects such as land destruction [1], environmental pollution [2,3], surface subsidence [4,5] and slope instability [6]. To alleviate the ground subsidence caused by coal mining, it is necessary to focus on the movement and fracture characteristics of overburden after coal mining [7–9], dynamic load response characteristics and fracture development mode after mining [10]. At present, the main research method for the above problems is analog physical simulation experiments [11]. In addition, analog physical simulation experiments are often used in the study of co-extraction of coal and gas [12].

Such research on analog materials was on two aspects: the proportion of rock–soil analog materials and the error analysis of the experimental process. The different cementation of analog materials was divisible into gypsum cementation [13] and cement cementation [14]. Some scholars developed new geotechnical analog materials according to the unique needs of coalbed methane, rock bursts, etc. [15,16]. Different mass ratios also made a significant impact on the strength of analog materials [17]. In terms of error analysis of analog simulation experiments, Luo [18] analyzed in detail the source of strength deviation of analog simulation materials under uniaxial compression.

Among various analog materials, gypsum-cemented analog materials were popular. Our team verified the influence of curing humidity and sand particle size on gypsum-cemented materials through experiments. Unfortunately, our experiments confirmed that gypsum-cemented analog materials generally need to be cured for more than 20 days

to reach the stable strength designed by the investigation [19,20]. As a result, it took a long time to complete an analog simulation experiment, which reduced the efficiency of the experiment. Therefore, it is essential to find a way to shorten the time of analog simulation experiments.

In recent years, with the advantages of high heating speeds, energy-saving, high efficiency, and low thermal inertia, microwaves have been widely used in various industries [21,22], such as food cooking [23], organic synthesis [24], environment engineering [25], coal drying [26,27], rock anti-reflection [28], etc. Therefore, it was a feasible idea to use the microwave for curing gypsum-cemented material to increase the hardening rate of the material. This article took gypsum-cemented analog simulation materials as the research object and used the same proportion scheme to study the relationship between the uniaxial compressive strength of gypsum-cemented analog materials and the microwave curing power and time. In addition, the mechanism of the strength variation of the gypsum-cemented analog materials under different curing conditions was explored through the measurement of temperature and moisture content, and scanning electron microscopy (SEM). Finally, the curing method that takes the least time to reach the design strength of gypsum-cemented material under microwave irradiation was determined, which provided a scientific basis for shortening the time of gypsum-cemented analog physical experiments.

2. Materials and Methods

2.1. Proportioning Materials

We used β-type hemihydrate gypsum ($CaSO_4 \cdot 0.5H_2O$), heavy stone powder ($CaCO_3$), and aeolian sand as the proportioning materials mixed with water to make the analog material. The gypsum used is the industrial gypsum is produced by Hebei Lingshou Shengyun Mineral Products Processing Plant Co., Ltd (Shijiazhuang, China). The calcium carbonate used is produced by Guangdong Jufu New Material Co., Ltd (Foshan, China). The aeolian sand used was obtained around Urumqi. As shown in Table 1, the strength of the original simulated rock was 79.5 MPa. According to the analog criterion [29] and test conditions (the height of the test frame was 2 m, the coal seam depth was 200 m), we determined the geometric ratio and the bulk density ratio to be 1/100 and 1/1.5, respectively. Then, the compressive strength of analog materials was 79.5 MPa/200/1.5 = 265 kPa. The proportion of analog materials was the optimal ratio obtained through continuous adjustment via many experiments [30]. Table 1 gives the specific proportions.

Table 1. Material proportioning plan for sample production.

Lithology	Density g/cm^3	Compressive Strength/MPa	Model Density g/cm^3	Model Compressive Strength/kPa	Hemihydrate Gypsum/%	Heavy Stone Powder/%	Sand/%	Water/%
Mudstone	1.68	39.7	1.12	265	9.5	8.1	72.4	10

2.2. Experiment Scheme

In order to facilitate the experiment, similar simulation materials are made into cylindrical specimens with a diameter of 5 cm and a height of 10 cm. After a large number of exploratory experiments in the early stage to explore the influence mechanism of microwave working conditions on the strength of analog materials and finally obtain the best curing conditions to identify the target strength of the materials in the shortest time, we designed three groups of experiments under three different power irradiation conditions as shown in Table 2. Each group had five different curing times and made five samples for each curing time and power condition, which made up 85 specimens. The stirring tool (see Figure 1a) helped stir the material's different components evenly. A standard sample mold (see Figure 1b), with a diameter of 5 cm and a height of 10 cm, was used to make standard samples. The lubricant was sprayed on the mold's inner surface before sample preparation to avoid the sample (see Figure 1c becoming damaged on mold removal). We adopted

the industrial microwave oven (see Figure 1d), supplied by the commercial microwave equipment manufacturer Newsail, for sample curing. The same personnel on the same day made all the samples, and the samples underwent microwave curing and experiments to minimize human error.

Table 2. Testing scheme to investigate the influence of microwave curing conditions on analog materials.

Group 1 (2000 W)		Group 2 (1200 W)		Group 3 (400 W)		Control Group	
Time/s	Number of Samples	Time/s	Number of Samples	Time/min	Number of Samples	Time/s	Number of Samples
0	5	0	5	0	5		
40	5	60	5	80	5		
80	5	120	5	160	5		
120	5	180	5	240	5	20d	5
160	5	240	5	320	5		
200	5	300	5	400	5		

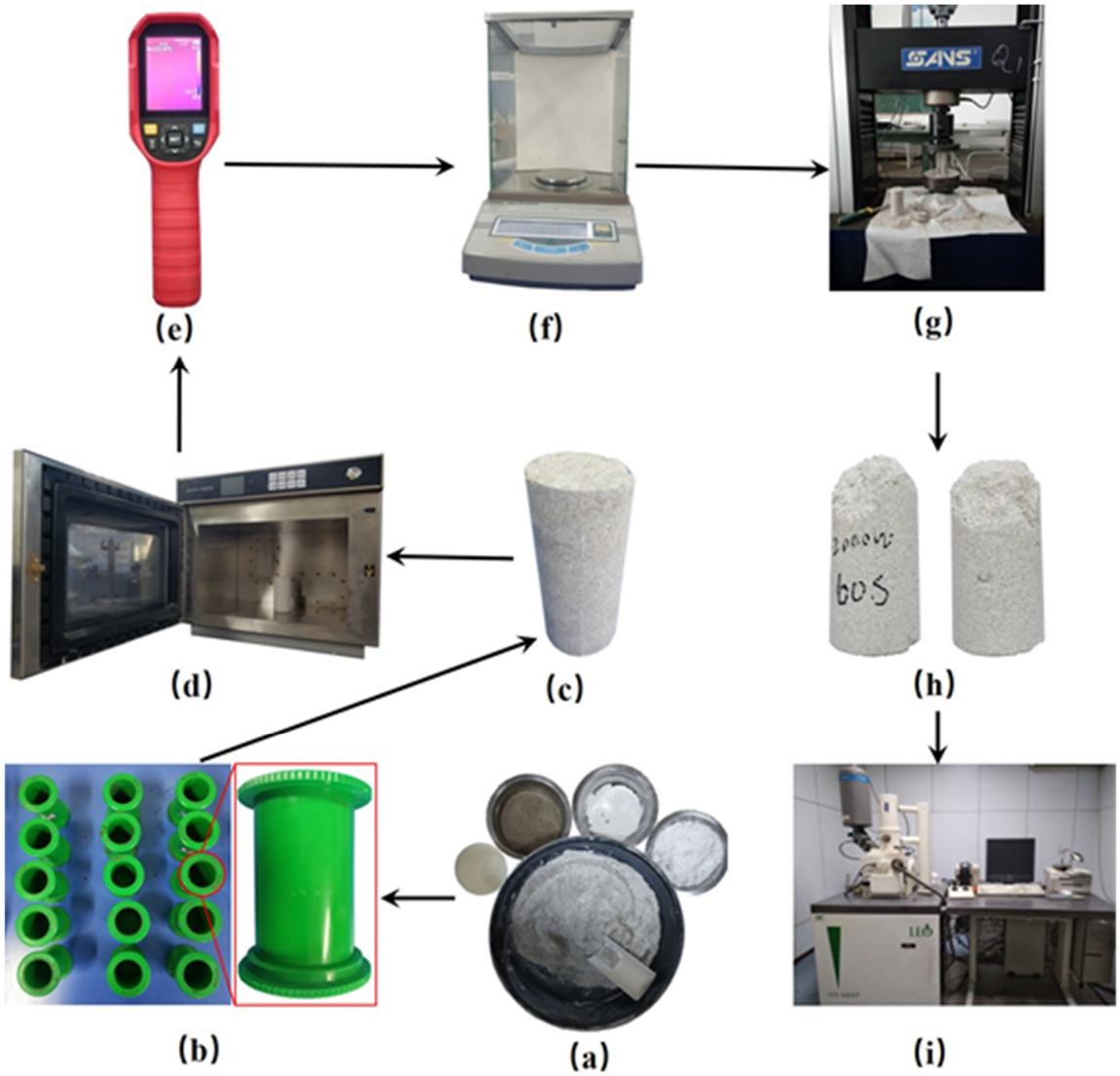

Figure 1. Instrumentation used in the research experiments. (**a**) Water, sand, gypsum, heavy stone powder, and mixing tools used to make standard specimens. (**b**) Molds used for making (**c**) standard samples. (**d**) Industrial microwave oven. (**e**) Handheld infrared thermal imager. (**f**) High-precision electronic balance. (**g**) Uniaxial Compressor. (**h**) Destroyed specimen. (**i**) SEM.

The variations in physical and mechanical properties, composition, and microstructure of analog materials cured under different microwave conditions, temperature, moisture content, and uniaxial compressive strength were measured and recorded immediately after each experiment. First, we measured the temperature of the sample with a UTi260B HD thermal imager produced by Uni-trend Technology Co., Ltd. (Shanghai, China), as shown in Figure 1e. Next, the overall moisture content of the specimen was determined with appropriate mass measurements of the specimen, using the FA2004N high-precision electronic balance produced by Shanghai Minqiao Precision Scientific Instrument Co., Ltd. (Shanghai, China), as shown in Figure 1f. Finally, the uniaxial compressive strength was measured using the uniaxial compression tester shown in Figure 1g. For each condition of curing power and time, randomly selected fragmented sample pieces for scanning electron microscopy (SEM) (see Figure 1i). When performing SEM, it was necessary to spray gold before observation due to the poor conductivity of sand and gravel materials.

3. Discussion and Results

3.1. Strength Variation of Microwave-Cured Analog Materials

The hydration reaction of the cement was the main reason for the formation of stable strength cemented analog materials. The hydration reaction comprised two phases: one was the new phases produced by the hydration reaction, the other was the residual phases that were not involved in the response or were residuals due to incomplete responses. Among them, what determined the strength characteristics of analog materials was a new phase, also known as the cement phase. For example, in gypsum-cemented analog materials, the cement phase is hemihydrate gypsum; the quantity, size, and spatial distribution determine the material's strength characteristics.

According to the existing research, the strength of gypsum-cemented material first increases rapidly with time and then slowly under natural curing conditions [17], reaching the stable strength after the 20th day, on completion of the gypsum hydration reaction.

However, we observed that the material's strength variation characteristics differed from that of natural curing through microwave curing experiments. As shown in Figure 2, the strength variation of the material versus curing time showed four stages. The first stage (section ab) was a slow growth stage, where the strength of the material increased at a slow rate. The second stage (section bc) was a rapid growth stage, where the strength of the material increased rapidly with the curing time, finally reaching the peak at point c. This strength was the peak strength under the curing condition. The third stage (section cd) was a rapid decline stage, where the strength of the material decreased rapidly over time. Finally, the fourth stage (section de) was the sound stage, where the material strength remained unchanged over time. The strength at this time was the stable strength of the material cured under this microwave power.

Although there were four stages in the strength variation process of materials under different microwave power curing conditions, there were still four differences between them (as seen in Figure 2): first, the peak strength was additional. The peak strengths under 2000 W, 1200 W, and 400 W microwave curing conditions were 171.6 kPa, 199.3 kPa, and 280 kPa, respectively, which showed a decreasing trend with microwave curing power. Second, the stable strengths were different. The stable strengths under 2000 W, 1200 W, and 400 W microwave curing conditions were 96.5 kPa, 131.2 kPa, and 266.5 kPa, respectively, which also decreased with microwave curing power. Third, the rates of strength growth were different, which slowed down as the microwave power fell. Under 2000 W, 1200 W, and 400 W microwave curing conditions, the time to reach the stable strength was 80 s, 120 s, and 200 min, and the time to gain the peak strength was 120 s, 240 s, and 300 min, respectively. The smaller the microwave power, the more time it took to reach the peak strength and the stable strength. Four, the difference between the peak strength and the continued strength of the material was different. Under 2000 W, 1200 W, and 400 W, microwave curing conditions were 75.1 kPa, 68.1 kPa, and 13.5 kPa. As the microwave curing power decreased, the strength difference decreased.

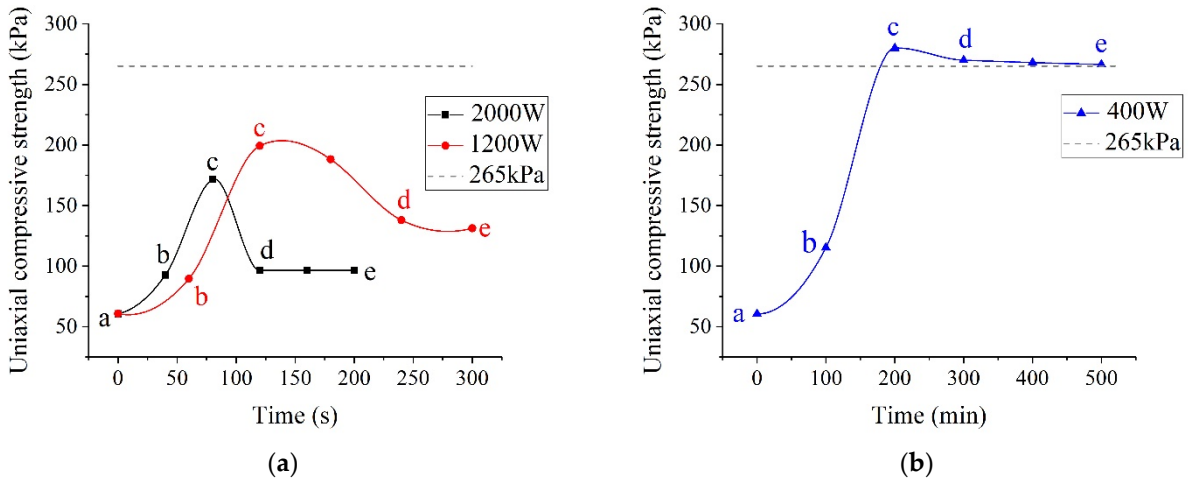

(**a**) (**b**)

Figure 2. Variation of the uniaxial compressive strength versus time. (**a**) Is the change of material strength with curing time under 1200 W and 2000 W curing conditions, (**b**) Is the change of material strength with curing time under 400 W curing conditions.

3.2. Strength Variation Mechanism of Microwave-Cured Analog Materials

Different microwave working conditions had two main effects on the strength of analog materials: strengthening and weakening. The factors that increased the strength of the material were: (1) the hydration of calcium sulfate hemihydrate generated calcium sulfate dihydrate, and the resulting dihydrate gypsum crystals were interwoven with each other, increasing the strength of the material, being the main reason for the stable strength of the material; (2) the reduction of moisture content improved the strength of the material. On the other hand, the factors that reduced the strength of the material were: (1) during microwave curing, the steam explosion effect of water vapor in the material voids made the voids more significant. The steam explosion was due to the rapid temperature increase of the water in the material voids, and the violent gasification in a short time produced a large amount of water vapor. However, the water vapor in the voids could not be discharged in time, leading to high water vapor pressure in the voids causing damage to the material [31]. (2) The thermal stress caused by the uneven temperature distribution at each point damaged the material. Thus, the two factors worked together to make the material strength show different characteristics under different microwave power conditions. Next, the influence of each factor was analyzed in the following sections.

3.2.1. Main Factors Affecting Material Strength

Temperature and moisture content were the main factors affecting material strength. Figure 3 shows the variation of material strength versus temperature and moisture content.

The main reasons why material moisture content affected material strength were, first, the decrease in moisture content increased the effective stress of the material and increased the friction angle of the material, which enhanced the material strength. Second, the free water in the material soaked the newly generated dihydrate gypsum. The free water will be physically adsorbed on the dihydrate gypsum crystals or exist independently in the specimen, forming the H_2O-$CaSO_4 \cdot 2H_2O$-H_2O structure. The interaction between H_2O and $CaSO_4 \cdot 2H_2O$ was fragile, which significantly reduced the material strength. Third, water had a high dielectric loss, and the main reason for the increase in material temperature was that the free water in the material absorbed a large amount of microwave energy. Therefore, reducing the moisture content weakened the material's ability to absorb microwaves, resulting in a slower heating rate.

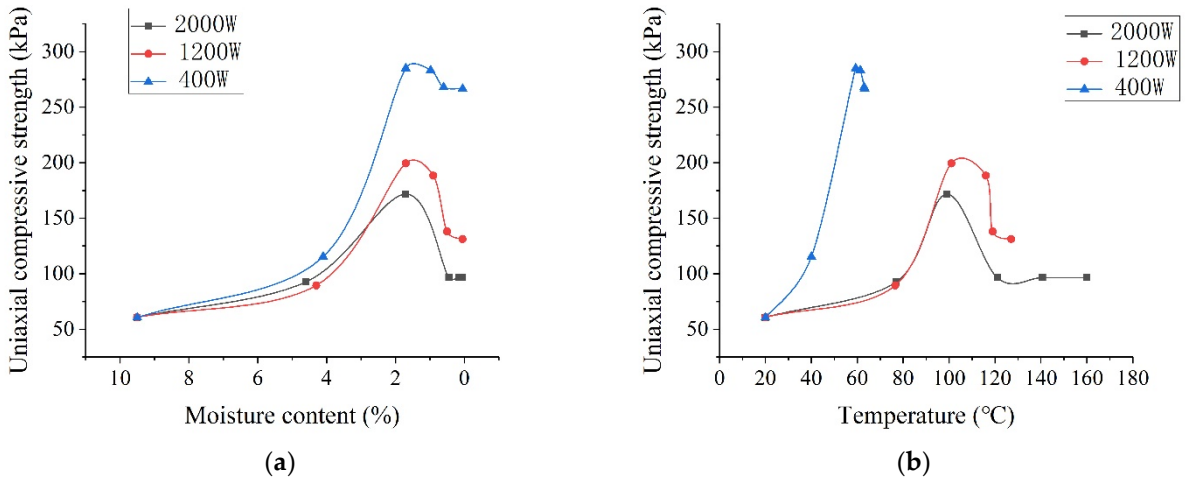

Figure 3. (**a**,**b**) The variations of uniaxial compressive strength versus temperature and moisture content, respectively.

There were four main reasons why temperature affected material strength. First, temperature affected the rate of hydration reaction of gypsum, which in turn affected the strength variation process of the material. As the microwave curing began, the hydration reaction of gypsum accelerated as the temperature rose. When the temperature increased above 40 °C, the hydration reaction rate decreased as the temperature rose. When the temperature reached above 100 °C, the hydration reaction of calcium sulfate hemihydrate to form calcium sulfate dihydrate stopped [32]. Second, the dielectric constant of water decreased as the temperature increased, therefore reducing the ability of water in the material to absorb microwaves. Hence, this was a further reason why the temperature increase rate of the material became progressively slower with the extension of the curing time. Thirdly, the increase in temperature sped up water evaporation and increased the rate of decrease in moisture content, which accelerated the rise in material strength. Fourth, the rapid temperature increased during the curing process and caused a steam explosion and thermal stress damage to the material. Due to the considerable difference in the dielectric loss of water and other media in the material, the temperature distribution at each point of the specimen during microwave heating was uneven, which in turn caused uneven thermal stress distribution. As a result, cracks appeared on the contact surface between gypsum cement and sand, extending and penetrating internally, resulting in decreased material strength. Figure 4 shows a 500 magnification SEM micrograph of the specimen used in this experiment, which intuitively indicated the voids formed by steam explosion and thermal stress.

3.2.2. The Mechanism That Affects the Variation of Material Strength

The preceding section analyzed how each factor affected the strength of gypsum cement material individually under microwave curing conditions. Thus, the four variation stages of the strength of the gypsum cementing material versus time in Figure 2 were the result of the simultaneous action of multiple factors. The following is a detailed analysis of how various aspects work together in stages, resulting in the different material strength characteristics versus time, as shown in Figure 2.

First, the slow growth stage (a–b): As shown in Figure 5, the material temperature at this stage increased drastically, while the moisture content decreased rapidly, and the strength of the material increased slowly. The increase in material strength at this stage was: (1) As the temperature increased, the rate of hydration reaction of gypsum increased. (2) As the moisture content of the material decreased, the effective stress and internal friction angle of the material increased. Thus, the two improved the mechanical strength of the material. At this time, the temperature was low, and the thermal stress and steam explosion effect of water vapor had no significant weakening effect on the strength. Therefore, the first

two factors became the main controlling factors at this stage, resulting in a slow upward trend of the material strength.

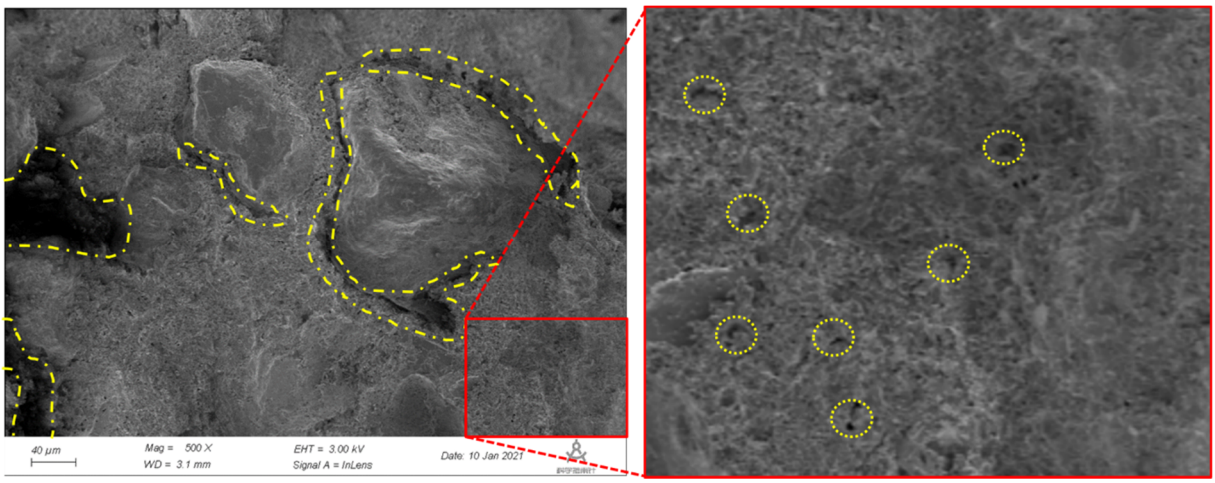

Figure 4. (**a**) The broken lines show the cracks that had penetrated. (**b**) The small circles show a small void that had not yet penetrated.

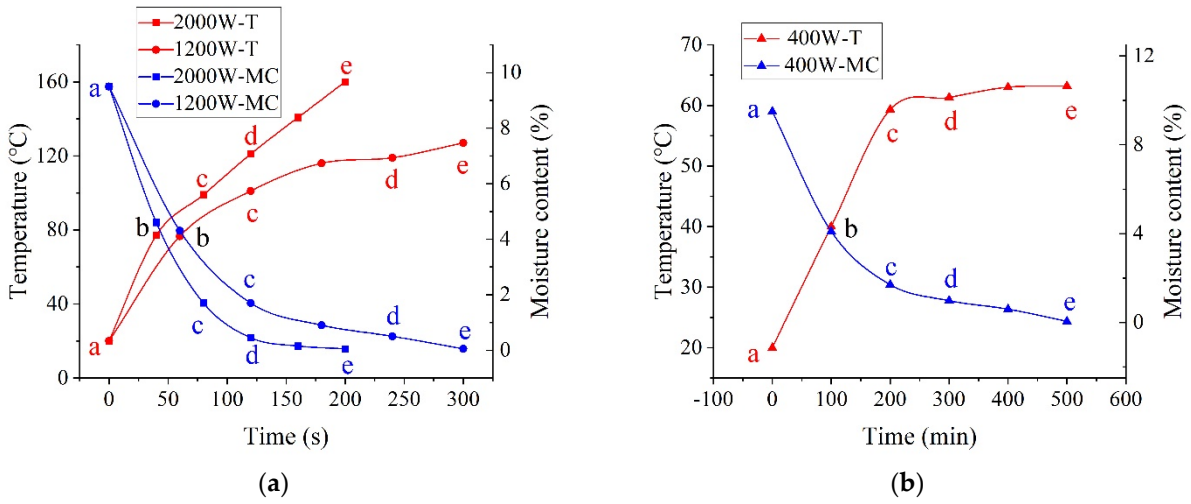

Figure 5. Variations of moisture content and temperature versus time. (**a**) is the relationship between the temperature and moisture content of the material with the curing time under the curing conditions of 1200 W and 2000 W. (**b**) is the relationship between the temperature and moisture content of the material with the curing time under the curing conditions of 400 W.

Secondly, the rapid growth stage (b–c): The material strength was also affected by the factors at the first stage. As shown in Figure 5, the material temperature at this stage had reached a relatively high level. The temperature ranges under 400 W, 1200 W, and 2000 W curing power conditions were 40–60 °C, 76–99 °C, and 77–103 °C, respectively. According to the hydration reaction theory of gypsum, under the curing condition of 400 W, the hydration rate of gypsum at this stage decreased, but the hydration reaction still went on. The hydration reaction rate under 1200 W and 2000 W conditions rapidly dropped to a deficient level at the beginning of this stage, which stopped later. Therefore, the hydration reaction of gypsum at this stage could not support the sharp increase in the material strength, which showed that the sharp rise in the material strength at this stage was mainly caused by the variation of the moisture content of the material. As shown in

Figure 5, at this stage, the moisture content under the conditions of 400 W, 1200 W, and 2000 W decreased from 4.1%, 4.3%, and 4.6% to 1.7%. It showed that when the moisture content of this gypsum cement material changed within this interval, it had a significant influence on the material strength.

Figure 5 shows that the temperature increase rate and the moisture content decrease rate of the material at this stage were slowing down, which was due to the following reasons: one was that the moisture content at this stage was less, and the ability of the material to absorb microwaves weakened, and the microwave energy absorbed per unit time became less, which causes the temperature rise of the material to slow down. Second, due to the increase in temperature, the dielectric constant of water was reduced, which also slowed down the heating rate of the material. The third was that, as the moisture content of the material decreased, the difference between the water content in the material and the atmosphere decreased, reducing the rate of water dissipation in the material.

Thirdly, the rapid reduction stage (c–d): At this stage, the main influencing factors under different power conditions were significantly different. As seen in Figure 5, the temperature of the material under microwave power of 2000 W and 1200 W had risen above 100 °C, stopping the hydration reaction of gypsum. Therefore, the material could no longer rely on the hydration reaction of gypsum to increase its strength. In contrast, with the 400 W curing condition, the temperature of the material increased from 59 °C to 61 °C, and the hydration reaction of gypsum still went on, contributing to the increase of material strength. Although the reduction of the moisture content can increase the material strength, as shown in Figure 5, the moisture content had dropped below 1.7% at this stage. Therefore, the moisture content decrease rate of the material had become very slow, which was very weak on strength.

However, as the temperature increased, the damage to the material caused by thermal stress and steam explosion intensified. As shown in Figure 6a–f, the SEM images of the material magnified 500 times clearly showed that under the three power microwave curing conditions, the number and size of voids of the material were more significant at the end of the stage than at the beginning. For a more precise analysis of the material voids, we statistically analyzed the void area percent and void size under the magnified 500 times SEM image, obtained and shown in Figure 7. The void area percentage at this stage was as follows: under 400 W conditions, it increased from 3.323% to 4.576%, an increase of 1.253%. Under 1200 W conditions, it grew from 6.302% to 13.516%, an increase of 7.214%. Under 2000 W conditions, it increased from 21.89% to 34.241%, an increase of 12.351%. At this stage, the average material void size is as follows: under 400 W conditions, it increased from 3.822 μm to 4.862 μm, increasing 1.04 μm. Under 1200 W conditions, it grew from 9.085 μm to 12.048 μm, an increase of 2.963 μm. Under 2000 W conditions, it increased from 20.841 μm to 23.000 μm, a rise of 2.159 μm. It was observed that under the same power condition, the material void number and size in this curing stage had a significant increase. It showed that, as the temperature increased to a higher level at this stage, the effect of steam explosion and thermal stress was intensified. These two effects led to an increase in the number and size of material voids, which even penetrated each other, leading to decreased material strength. The number and the size of voids of materials under different power microwave curing conditions were very different. The higher the microwave power, the greater was the number and the size of the voids of the cured material, and more significant also was the increase in the size and the number of voids at this stage.

Fourth, overall stable stage (d–e): When entering this stage, as seen in Figure 5, the variations in moisture content and temperature further slowed down, and the influence of moisture content on the material strength further weakened. At this stage, the moisture content had reached a reasonably low level, so the ability of the sample to absorb microwaves at this stage was fragile. As a result, the temperature of the sample increased slowly, and the temperature difference at each point of the sample became minimal, resulting in the slight effect of thermal stress on the material strength. Similarly, due to the extremely low water content, the steam explosion effect in the material was non-existent. Therefore, the

impact of the steam explosion did not affect the material strength at this time. Therefore, the material strength at this stage remained unchanged regardless of the curing power. Thus, at this time, the cured material had reached stable strength under the curing condition.

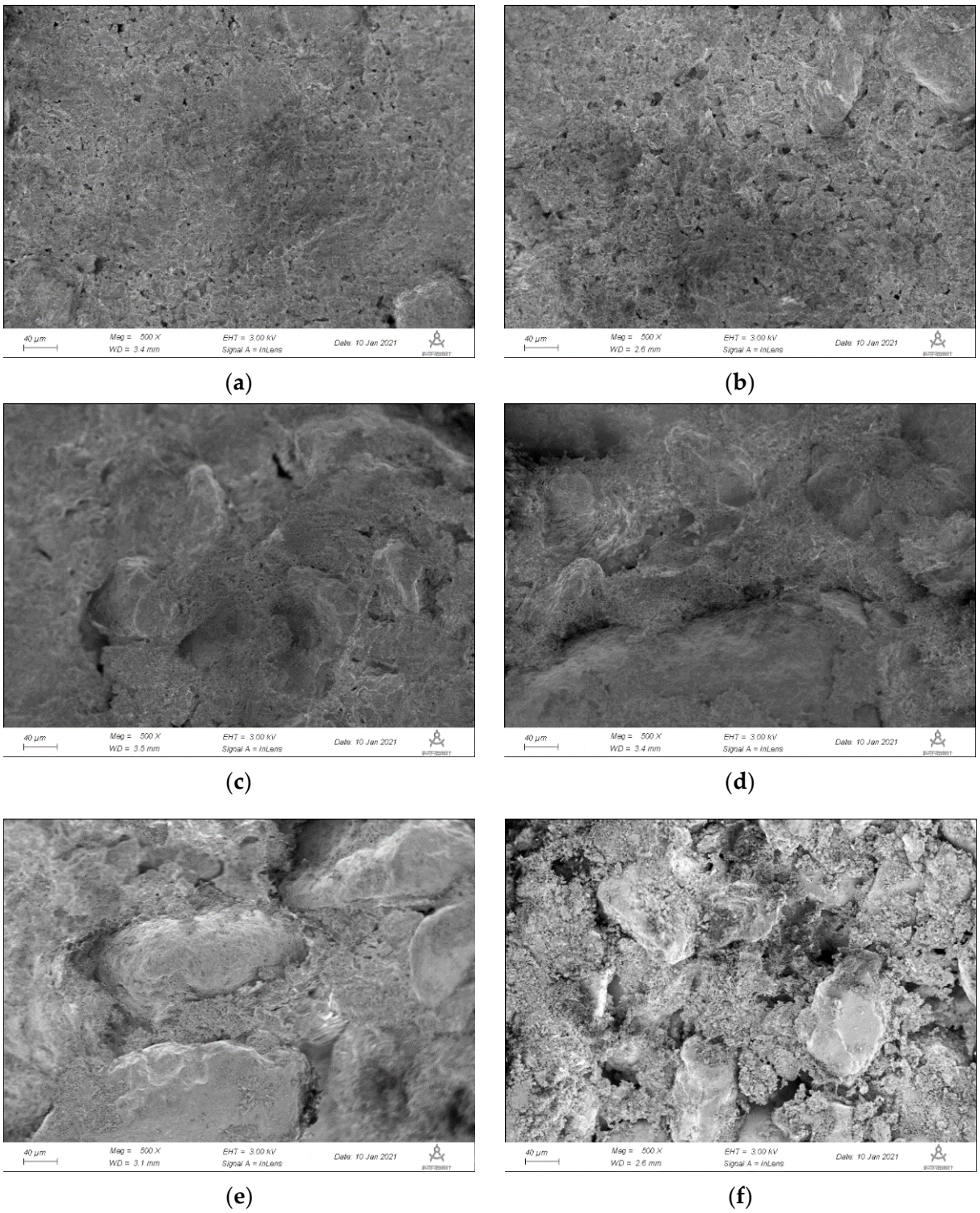

Figure 6. Void distribution within the material. (**a**) 400 W 200 min, (**b**) 400 W 300 min, (**c**) 1200 W 120 s, (**d**) 1200 W 240 s, (**e**) 2000 W 80 s, (**f**) 2000 W 120 s.

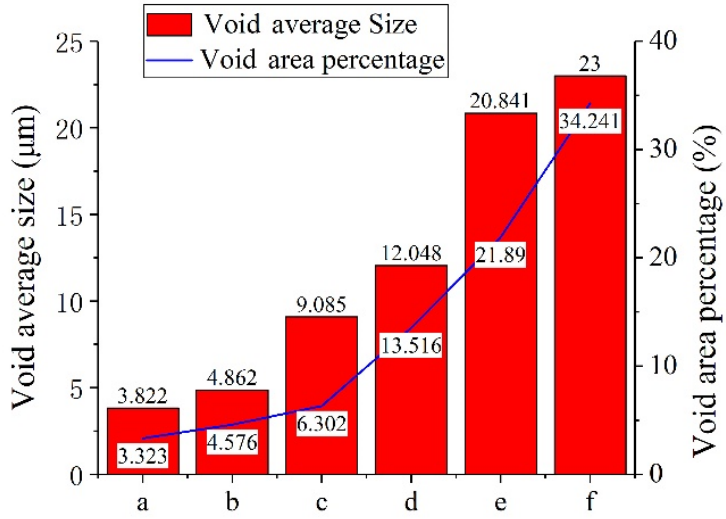

Figure 7. Void statistics. (a—400 W 200 min, b—400 W 300 min, c—1200 W 120 s, d—1200 W 240 s, e—2000 W 80 s, f—2000 W 120 s).

3.3. Irradiation Condition Control Method of Microwave-Cured Analog Materials

The previous section proved through experiments the pattern of material strength variation versus microwave curing time under different power conditions, and compared the magnitude relationship of the strength at each stage under other power conditions. We concluded that the higher the microwave power, the more violently the material strength increased and the shorter the time it took to complete a strength development stage. However, no matter the stage of variation, the higher the power, the lower the material's strength was. Figure 8 shows the comparison between the stable material strength under various power conditions with the strength on the 20th day under natural curing conditions (265 kPa). We also observed that the progressive strength of gypsum-cemented material under 400 W microwave curing was the closest to the resilience of natural curing for 20 days, while the continued strength of the material under 1200 W and 2000 W conditions was far lower than that of naturally cured material.

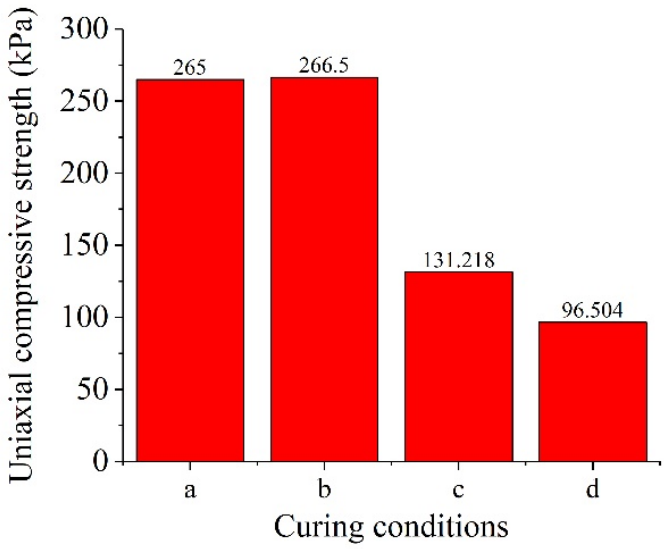

Figure 8. The uniaxial compressive strength statistics of materials, where a is natural curing for 20 days, b is curing under 400 W microwave conditions for 500 min, c is curing under 1200 W microwave conditions for 300 s, and d is curing under 2000 W microwave conditions for 200 s.

The reason was that the dielectric constant of each medium in the material was very different. The higher the power, the more microwave energy, the more significant the temperature difference inside the specimen, and the more severe the damage to the material by the induced thermal stress. In addition, the higher the microwave power, the more intense the vaporization of the moisture in the material, and the more severe the steam explosion. Figure 8 is an SEM picture of the specimen magnified 10,000 times. It was seen that the dihydrate gypsum crystals under high-power microwave curing were less than the dihydrate gypsum crystals under natural curing and low-power microwave curing conditions. The higher the microwave power, the fewer dihydrate gypsum crystals formed because when the microwave power was high, the material reached a very high temperature in a short time, which quickly exceeded the upper limit of the microwave gypsum hydration reaction temperature. As a result, the hydration reaction time of gypsum was short, and the growth of dihydrate gypsum crystals was minimal. Therefore, the development of dihydrate gypsum crystals had minimal effect on the strength of the material. However, under the condition of high microwave power, the moisture content of the material decreased rapidly in a short time, which increased the strength of the material rapidly.

In summary, under the condition of high-power microwave curing, the strength of gypsum-cemented material rapidly improved with the rapid reduction of moisture content. However, due to the strong effect of steam explosion and thermal stress, the number and size of material voids increased, and the cracks at the interface between gypsum and sand particles grew, expanded, and penetrated. It results in a significant reduction in the strength of the materials. Coupled with the low degree of gypsum hydration reactions, the stable strength of the material was much lower than the strength of the gypsum-cemented material cured for 20 days under natural conditions.

On the contrary, as shown in Figure 5, under low-power microwave conditions, the temperature reached the more suitable temperature for gypsum hydration reactions. It maintained the temperature for a long time so that hemihydrate gypsum quickly underwent a hydration reaction to form dihydrate gypsum crystals. Coupled with the material strength increase due to the decrease in moisture content, the strength of the material significantly improved in a relatively short time. Compared with specimens cured under natural conditions for 20 days, the strength of specimens cured under 400 W microwave was very close but with a slight difference in crystal morphology. As shown in the SEM image in Figure 9, the crystals of calcium sulfate dihydrate under the conditions of 400 W microwave curing were more slender, mostly needle-shaped, with a length of 3–7 μm and a diameter of 0.2–0.4 μm.

In contrast, the calcium sulfate dihydrate crystals under constant temperature curing were coarser and shorter, mainly in the form of flakes, with a length of 2–7 μm and a diameter of 0.3–2.5 μm. From the perspective of crystal morphology alone, the more slender cementing crystal material under low-power microwave conditions generally had higher mechanical strength. However, from the experimental results, the strength of the specimens under the two conditions were very close because steam explosion and thermal stress reduced the strength of the material during the microwave curing process, which offset the increased strength of the material due to the crystal form of dihydrate gypsum. As shown in Figure 10, comparing the materials under 400 W microwave curing for 500 min with that of natural curing for 20 days, the number and size of material voids under 400 W conditions were more significant than those under natural curing. According to statistics, the void area percentage of the material cured under natural conditions for 20 days was 2.127%, and the average size was 3.71 μm, while the void area percentage of the material cured by 400 W microwave for 500 min was 4.876%, and the average size was 4.92 μm.

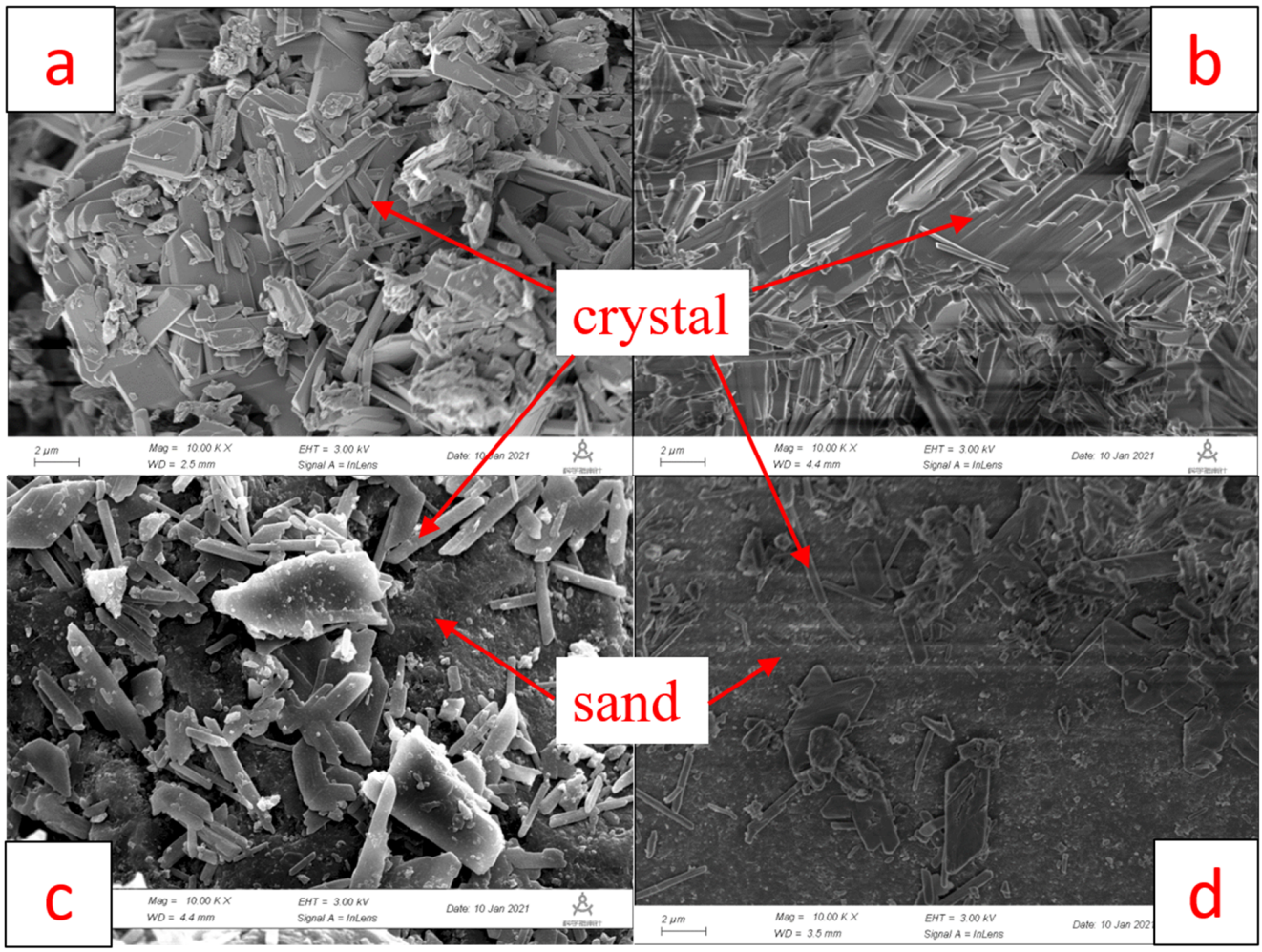

Figure 9. Crystal morphology magnified 10,000 times under the scanning electron microscope. (**a**) Natural 20-day curing condition; (**b**) 400 W–500 min curing condition; (**c**) 1200 W–300 s curing condition; (**d**) 2000 W–200 s curing condition.

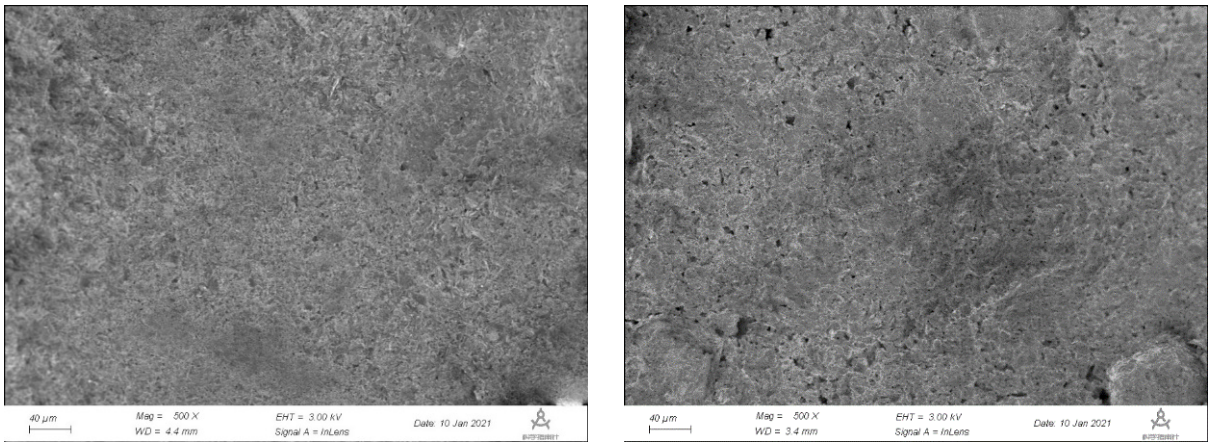

(**a**) (**b**)

Figure 10. Comparison of void conditions under natural curing and 400 W microwave curing conditions. (**a**) Natural curing for 20 days; (**b**) microwave 400 W curing for 500 min.

There are three reasons for the different crystal forms of calcium sulfate dihydrate crystals formed by the hydration reaction of gypsum under microwave curing and natural

curing. First, after the reactants and products absorb the microwave under the action of the microwave, the speed of molecular motion increases. It makes the molecules change 2.45×10^9 times per second according to the direction and intensity of the electronic field, causing a lot of friction of the molecules and thus increases the temperature of the system. As a result, the specific surface energy of the crystal interface becomes smaller, and the nucleation rate becomes more extensive. Second, in the process of crystal growth under microwave irradiation, polar molecules continue to perform molecular orientation after absorbing microwaves, which changes the structure of the solution near the crystal surface.

Moreover, the friction between the crystal or the liquid phase was intensified, and there were also molecular and particle-level collisions between particles and particles, between particles and solution, and between solution molecules and solvent molecules. This effectively prevented the formation of agglomerates, increased the number of growing crystals, reduced particle size, and promoted contact nucleation. Thirdly, due to the strong polarity of water molecules, microwave action weakened the solvent's hydrogen bond, increased the degree of ionization, and changed the solvent's structure. As a result, the ability of the crystal solute to diffuse to the crystal phase interface improved, and the collision probability of the solute reaching the crystal surface with the crystal also increased. These effects promoted the acceleration of the crystallization rate.

In summary, although high-power (2000 W and 1200 W) microwave curing conditions achieved high strength quickly, the material's design strength was also not reached. On the contrary, the low-power (400 W) microwave curing of gypsum-cemented material gained the strength of natural curing for 20 days in a short time (500 min). Furthermore, it showed that low-power microwave curing could significantly shorten the time of similar physical tests of gypsum cementation, so that the experiment that initially took 20 days to complete was completed in less than a day, saving a lot of time.

3.4. Intelligent Devices for Microwave Irradiation

To test the feasibility of the microwave irradiation curing method and put the theoretical results of this paper into practice, this paper designed and manufactured a complete set of intelligent devices for curing the gypsum-cemented analog material models, as shown in Figure 11. The feature of this device is that it can measure the humidity and temperature of analog materials through the humidity and temperature sensors embedded in the analog materials model, and automatically adjust the microwave irradiation mode according to the moisture and temperature of the material, so that the temperature of the material is maintained between 40 °C and 60 °C. In this way, the gypsum maintained a high hydration reaction rate, thereby speeding up the curing process of the gypsum-cemented analog materials. Furthermore, when the humidity was lower than 1% (as shown in Figure 6, when the material humidity was less than 1%, the material strength remains unchanged), microwave irradiation stopped. Thus, no manual intervention was necessary during the whole curing process.

This smart device was used to cure the gypsum-cemented analog materials model with the size of 0.5 m × 0.5 m, as shown in Figure 11b, and the proportioning was precisely the same as the experiment in the previous sections of this paper. Furthermore, the results show that it takes more time to cure the real simulation model to reach the standard strength than 400 W microwave curing cylindrical specimens to reach the same strength; however, it is much shorter than natural curing to reach the same strength. This shows that the method of cementing similar material models with microwave curing gypsum is feasible. However, further research is needed to optimize the irradiation method.

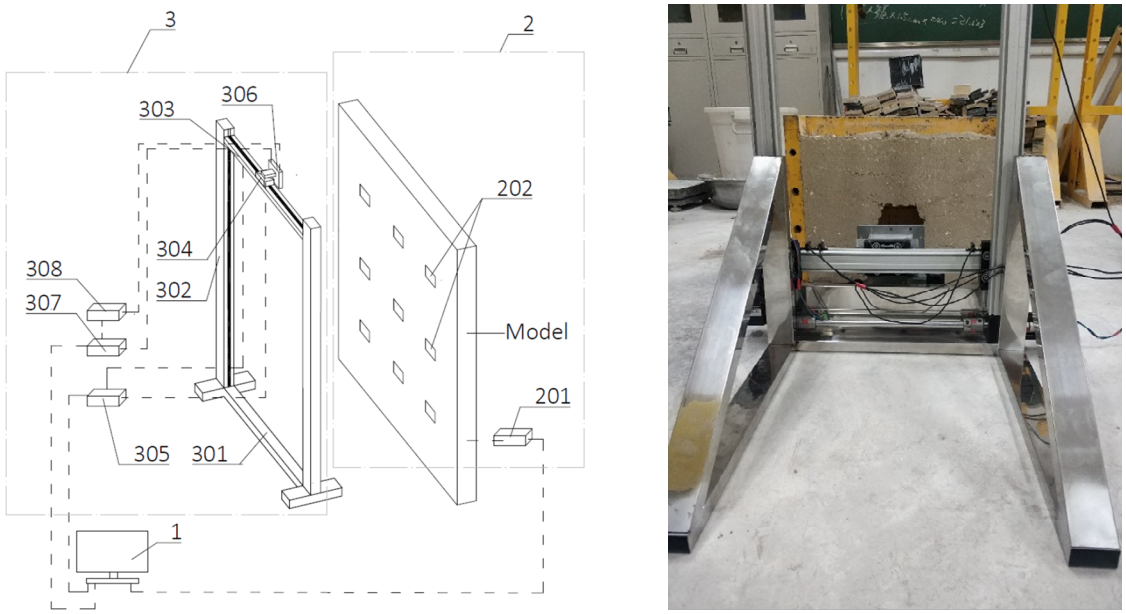

(**a**) (**b**)

Figure 11. (**a**) Schematic diagram of the structure of the intelligent device. 1. Master controller; 2. Humidity and temperature monitoring system; 3. Mobile microwave irradiation system; 201. Humidity and temperature signal processor; 202. Humidity and temperature-sensitive components; 301. Base; 302. Vertical chute; 303. Horizontal conduit; 304. Load slide; 305 Displacement driver; 306. Microwave generator; 307. microwave controller; 308. microwave adapter power supply. (**b**) A physical image of the smart device.

4. Conclusions

In this paper, through the microwave curing experiment, the variation laws of temperature, moisture content and uniaxial compressive strength of specimens under different microwave curing power and curing time are compared and analyzed, and the influence mechanism of microwave curing conditions on similar materials is clarified. Finally, the experimental control method of rapid strengthening of gypsum-cemented similar materials by microwave field control is obtained, and the microwave irradiation device for curing the actual similar material model is preliminarily set up. At the same time, the following conclusions are obtained:

(1) The strength of gypsum-cemented material under microwave irradiation had four variation stages versus the curing time: slow growth, rapid growth, rapid decrease, and overall stability. In addition, the smaller the microwave power, the smaller the difference was between the strength of the sound stage and the maximum strength during the curing process, and the greater the stable strength of the material.

(2) Under high-power microwave curing, the improvement of material strength mainly depended on the loss of water in the material, which increased the material's effective stress and internal friction angle, thereby increasing the strength of the material.

(3) The more significant the microwave irradiation power, the lower the cured material's strength. The reason was that when the temperature was too high, steam explosion and thermal stress damaged the material and reduced the strength of the material.

(4) The strength of the material obtained by 400 W microwave curing was very close to the strength of the material under natural curing, but the curing time was only 1/60 of that under natural curing conditions. Thus, it showed that it was entirely feasible to use low-power microwave irradiation to shorten the curing time of gypsum-cemented analog simulation materials.

(5) Although the strength of the material under low-power microwave curing and natural curing conditions was similar, the crystal form of calcium sulfate dihydrate was different, caused by the unique effect of microwaves on materials.

(6) Through the experimental verification results of the microwave irradiation intelligent device, it was suggested that it is feasible to use the microwave irradiation smart device to cure the gypsum-cemented similar material model designed and manufactured in this paper to shorten the experimental time.

However, when using the microwave irradiation device to cure the real analog model, it will be affected by other factors other than maintenance power and time, such as model size, moving speed of the microwave generator, and distance from the microwave generator to the model. Therefore, our team will conduct in-depth research on the above influencing factors at a later stage.

Author Contributions: Conceptualization, S.N.; methodology, W.G. and S.N.; software, W.L., H.L. and H.Z.; validation, Y.W. and J.Y.; data curation, W.G. and S.N.; writing—original draft preparation, W.G. and S.N.; writing—review and editing, S.N. All authors have read and agreed to the published version of the manuscript.

Funding: This research was funded by the National Natural Science Foundation of China, grant number 51764050; and the National Undergraduate Innovation and Entrepreneurship training program of China, grant number 202110755003.

Data Availability Statement: The data presented in this study are available from the corresponding author upon a reasonable request.

Conflicts of Interest: The authors declare no conflict of interest.

References

1. Li, Y.; Chiu, Y.H.; Lin, T.Y. Coal production efficiency and land destruction in China's coal mining industry. *Resour. Policy* **2019**, *63*, 101449. [CrossRef]
2. Qi, R.; Liu, T.; Jia, Q. Simulating the sustainable effect of green mining construction policies on coal mining industry of China. *J. Clean. Prod.* **2019**, *226*, 392–406. [CrossRef]
3. Wang, Y.; Lei, Y.X.; Wang, S.Y. Green mining efficiency and improvement countermeasures for China's coal mining industry. *Front. Energy Res.* **2020**, *8*, 18. [CrossRef]
4. Zhang, D.S.; Fan, G.W.; Wang, X.F. Characteristics and stability of slope movement response to underground mining of shallow coal seams away from gullies. *Int. J. Min. Sci.* **2012**, *22*, 47–50. [CrossRef]
5. Xia, Y.C.; Zhi, J.F.; Sun, X.Y. Study on relation between tectonic stress and coalmining subsidence with analog material simulation. *J. Coal Sci. Eng.* **2005**, *11*, 37–40.
6. Tao, M.; Chen, X.; Ding, Q.Q. A method for subsidence monitoring of similar material simulation test in coal mining. *Adv. Mater. Res.* **2013**, *765*, 2172–2175. [CrossRef]
7. Wang, X.F.; Zhang, D.S.; Fan, G.W. Underground Pressure Characteristics Analysis in Back-gully Mining of Shallow Coal Seam Under a Bedrock Gully Slope. *Min. Sci. Technol.* **2011**, *21*, 23–27. [CrossRef]
8. Wang, F.T.; Zhang, C.; Zhang, X.G.; Song, Q. Overlying strata movement rules and safety mining technology for the shallow depth seam proximity beneath a room mining goaf. *Int. J. Min. Sci. Technol.* **2015**, *25*, 139–143. [CrossRef]
9. Wen, B.A.; Yan, Y.; Dong, Y.X. The application of analog material in the simulation of overlying strata movement in high inclined seam in Dong Baowei mine. *Adv. Mater. Res.* **2012**, *600*, 194–198. [CrossRef]
10. Yan, S.Y.; Yang, K.; Liao, B.C. Experimental study of high mining-induced stress evolution characteristics of downward relieving mining in Paner coal mine. *Rock Soil Mech.* **2013**, *34*, 2551–2556.
11. Zhang, H.W.; Han, J.; Hai, L.X. Study on closed multiple-seam in the ascending mining technology. *J. Min. Saf. Eng.* **2013**, *30*, 63–67.
12. Hu, Q.; Zhang, S.; Wen, G. Coal-like material for coal and gas outburst simulation tests. *Int. J. Rock Mech. Min. Sci.* **2015**, *74*, 151–156. [CrossRef]
13. Li, J.G.; Wu, Y.; Wang, Y.Y. Experimental study on self-made similar material of soft rock. *Key Eng. Mater.* **2017**, *717*, 140–146. [CrossRef]
14. Yang, R.S.; Zhang, Y.F.; Yang, L.W. Study on the mixing proportion test of similar material gypsum. *China Min. Mag.* **2013**, *22*, 125–130.
15. Jiang, Y.Z.; Wang, R.H.; Tang, T.C. Research on plane strain model test of rockburst of underground cavern in hard brittle rockmass. *Appl. Mech. Mater.* **2018**, *102*, 1539–1556. [CrossRef]

16. Zhao, P.X.; Li, S.G.; Zhuo, R.S. Experimental research on the properties of "solid-gas" coupling physical simulation analog materials and testing by computer of gas in coal rock. *Wirel. Pers. Commun.* **2018**, *102*, 1539–1556. [CrossRef]
17. Liu, Y.S.; Li, J.; Wu, Q.L. Sensitivity analysis and proportioning design of rock burst similar materials. *Funct. Mater.* **2017**, *24*, 496–500. [CrossRef]
18. Cheng, W.M.; Sun, L.; Wang, G. Experimental research on coal seam analog material proportion and its application. *Int. J. Min. Sci. Technol.* **2016**, *26*, 913–918. [CrossRef]
19. Guan, W.M.; Qi, Q.; Zhang, Z.Y. Effect of Sand Particle Size on Microstructure and Mechanical Properties of Gypsum-Cemented Similar Materials. *Materials* **2020**, *13*, 765. [CrossRef]
20. Guan, W.M.; Zhang, D.S.; Wen, Y.Y. Influence of curing humidity on the compressive strength of gypsum-cemented similar materials. *Adv. Mater. Sci. Eng.* **2016**, *2016*, 7062624. [CrossRef]
21. Metaxas, A.C. Microwave heating. *Power Eng. J.* **1991**, *5*, 237–247. [CrossRef]
22. Meredith, R.J. *Engineers' Handbook of Industrial Microwave Heating*; The Institution of Engineering and Technology: London, UK, 1998.
23. Oliveira, M.E.; Franca, A.S. Microwave heating of foodstuffs. *J. Food Eng.* **2002**, *53*, 347–359. [CrossRef]
24. Kappe, C.O. Controlled microwave heating in modern organic synthesis. *Angewandte Chemie* **2004**, *43*, 6250–6284. [CrossRef]
25. Jones, D.A.; Lelyveld, T.P.; Mavrofidis, S.D. Microwave heating applications in environmental engineering—A review. *Resour. Conserv. Recycl.* **2002**, *34*, 75–90. [CrossRef]
26. Pickles, C.A.; Gao, F.; Kelebek, S. Microwave drying of a low-rank sub-bituminous coal. *Min. Eng.* **2014**, *62*, 31–42. [CrossRef]
27. Song, Z.; Jing, C.; Yao, L. Microwave drying performance of single-particle coal slime and energy consumption analyses. *Fuel Process. Technol.* **2016**, *143*, 69–78. [CrossRef]
28. Qi, Q.; Guan, W.M.; Li, X. Mechanism of Increasing the Permeability of Water-Bearing Coal Rock by Microwave Steam Explosion. *Geofluids* **2021**, *2021*, 6661867. [CrossRef]
29. Li, G.; Ma, F.S.; Guo, J. Experimental Study on Similar Materials Ratio Used in Large Scale Engineering Model Test. *Nat. Sci.* **2020**, *41*, 1653–1660.
30. Zhang, X.Y.; Luo, L.; Xu, L.F. Research on Quantitative Determination Method of Similar Materials Ratio. *Saf. Coal Mines* **2019**, *50*, 45–53. [CrossRef]
31. Fletcher, D.F. Steam explosion triggering: A review of theoretical and experimental investigations. *Nucl. Eng. Des.* **1995**, *155*, 27–36. [CrossRef]
32. Comel, C.; Karmazsin, E.; Murat, M. Theoretical interpretation of the existence at 35 °C of an absolute maximum of the hydration rate of calcium sulfate hemihydrate. *Thermochim. Acta* **1979**, *31*, 71–77. [CrossRef]